Carbohydrate Polymers 96 (2013) 57–63

Contents lists available at SciVerse ScienceDirect

Carbohydrate Polymers

journal homepage: www.elsevier.com/locate/carbpol

Effect of clay concentration on morphology and properties of hydroxypropylmethylcellulose films

Dibyendu Mondal[a], Biplab Bhowmick[a], Md. Masud R. Mollick[a], Dipanwita Maity[a], Asis Mukhopadhyay[b], Dipak Rana[c], Dipankar Chattopadhyay[a,*]

[a] Department of Polymer Science and Technology, University of Calcutta, 92 A.P.C. Road, Kolkata 700 009, India
[b] Department of Jute and Fiber Technology, Institute of Jute Technology, University of Calcutta, 35 Ballygunge Circular Road, Kolkata 700 019, India
[c] Department of Chemical and Biological Engineering, Industrial Membrane Research Institute, University of Ottawa, 161 Louis Pasteur St., Ottawa, ON K1N 6N5, Canada

ARTICLE INFO

Article history:
Received 8 January 2013
Received in revised form 11 March 2013
Accepted 20 March 2013
Available online 28 March 2013

Keywords:
Hydroxypropylmethylcellulose
Nanocomposites
Mechanical properties
Moisture absorption and water vapor permeability

ABSTRACT

Hydroxypropylmethylcellulose (HPMC)/montmorillonite (MMT) nanocomposite films are prepared by solution intercalation method. Mechanical, thermal, moisture absorption, optical clarity and water vapor permeability of HPMC/MMT nanocomposite films are measured. X-ray diffraction (XRD) and transmission electron microscopic (TEM) results establish formation of partially intercalated and partially exfoliated HPMC/MMT nanocomposite films. In presence of MMT, the tensile strength, tensile modulus and elongation at break of HPMC films are improved. The thermal stability of HPMC/MMT nanocomposites is better than pure HPMC. The moisture absorption of HPMC film measured in 75% of constant relative humidity is reduced with loading of MMT. Optical clarity of HPMC film is almost unaffected in presence of MMT. Water vapor permeability of HPMC decreases in presence of nanoclay due to increasing tortuous path for diffusion.

1. Introduction

In recent years, the application of biodegradable polymers increases to avoid uses of non biodegradable synthetic polymers from petroleum source which give rise to environmental problems. But biodegradable polymers such as methylcellulose, hydroxypropylmethylcellulose, starch, lignin, cellulose acetate, poly(vinyl alcohol) (PVA) and polyester have lower mechanical, barrier, water resistance properties and thermal properties compare to synthetic polymers. Therefore, to replace non biodegradable petrochemical synthetic polymers by biodegradable polymers, properties of biodegradable polymers are to be improved by several methods such as blending with synthetic polymers (Arvanitoyannis, Biliaderis, Ogawa, & Kawasaki, 1998; Bhattacharya, 1998) or natural polymers (Coffin, Fishman, & Cooke, 1995; Xu, Kim, Hanna, & Nag, 2005) or by adding nanofillers such as various types of clays (Tang & Alavi, 2012) and also by crosslinking (Simkovic, Laszlo, & Thompson, 1996).

Development of biodegradable polymers/clay nanocomposites is the most importance step towards enhancement of properties such as mechanical, thermal and barrier (Yang, Wang, & Wang, 2007). Sodium montmorillonite (MMT) type of layer silicates clay is the most widely used nanofiller in polymer nanocomposites. Montmorillonite is an octahedral alumina sheet sandwiched between two tetrahedral silica sheets (Ray & Bousmina, 2005). Polymers and layer silicates clay particles interact by different ways (Tunç & Duman, 2007). Ionic polymers are adsorbed on the surface of clay particles by electrostatic interactions, while non-ionic polymers adsorb by steric interactions.

Polymer/clay nanocomposite materials have widely been studied in the past. The synthesized starch/montmorillonite composite films with enhanced physical properties have shown poor water vapor transmission rate and moisture absorption (Kampeerapappun, Aht-ong, Pentrakoon, & Srikulkit, 2007). Water vapor permeability or gas permeability is a very essential property for various applications. Rimdusit, Jingjid, Damrongsakkul, Tiptipakorn, and Takeichi (2008) studied the thermal, tensile properties and biodegradability of MC/MMT nanocomposites as well as MC-gluteraldehyde crosslinked films. Tunç and Duman (2010) prepared MC/MMT nanocomposite films by different methods for food packaging applications. Preparation and characterization of chitosan/montmorillonite nanocomposite is reported by Wang et al. (2005). Nanocomposites of cellulose acetate and sodium montmorillonite are prepared using the solution intercalation method with different solvents by Romero, Leite, and Gonçalves

* Corresponding author. Tel.: +91 33 2350 1397/6996/6387/8386; fax: +91 033 2351 9755.
E-mail address: dipankar.chattopadhyay@gmail.com (D. Chattopadhyay).

0144-8617/$ – see front matter © 2013 Elsevier Ltd. All rights reserved.
http://dx.doi.org/10.1016/j.carbpol.2013.03.064

(2009). Chang, Jang, Ihn, Lee, and Sur (2003) studied the thermal and tensile properties of PVA hybrids with various clays: Na ion-exchanged clays and alkyl ammonium ion-exchanged clays.

Hydroxypropylmethylcellulose (HPMC) is a biodegradable and biocompatible polymer. Although, optical clarity of HPMC film is far better compare to methylcellulose (MC) film but till date there is no report on HPMC/MMT nanocomposite film. So, we have selected HPMC for making nanocomposite films with MMT.

In this work, hydroxypropylmethylcellulose (HPMC)/MMT nanocomposite films are prepared by solution intercalation process. The nanocomposites of HPMC/MMT are characterized by X-ray diffraction (XRD), transmission electron microscopy (TEM), thermo gravimetric analysis (TGA), and water vapor transmission rate (WVTR). Mechanical properties, optical clarity and moisture absorption of nanocomposite films are also measured.

2. Experimental

2.1. Materials

Hydroxypropylmethyl cellulose (HPMC) (50 cps) was purchased from Central Drug House (P) LTD, New Delhi, India. Unmodified montmorillonite clay (MMT) was obtained from nanocor, Sigma Aldrich with a cation-exchange capacity of 100 mequiv/100 g.

2.2. Preparation of HPMC/MMT nanocomposite films by solution mixing process

HPMC/MMT nanocomposites were prepared by solution mixing process. Suspensions of MMT were prepared by dispersing MMT in distilled water. 1 g HPMC was added in MMT suspension at room temperature with continuous stirring for 12 h and followed by sonication for 30 min. Then, solutions were transferred into glass plate at room temperature. Thin films of appropriate thickness were obtained after evaporation of water.

3. Characterizations

3.1. X-ray diffraction (XRD)

X-ray diffraction (XRD) analysis of the nanocomposite samples were performed at room temperature by X-PERT-PRO Panalytical diffractometer using Cu Kα (λ = 1.5406) as X-ray source at a generator voltage of 40 kV and current of 30 mA. The scanning rate was 1°/min. From XRD data, the interlayer spacing of clay platelets was calculated using Bragg's law as follows:

$$d = \frac{\lambda}{2\sin\theta} \quad (1)$$

where d is d-spacing (nm), λ is wavelength of X-ray beam (nm), and θ is the angle of incidence.

3.2. Transmission electron microscopy (TEM)

The nanoscale morphology of the HPMC/3 wt%MMT nanocomposites was observed by using transmission electron microscope (TEM). TEM was performed on a high resolution TEM (HRTEM) (model: JEM 2010 EM) at 120 kV accelerated voltage.

3.3. Mechanical properties

The mechanical properties of the solution cast HPMC and its nanocomposite films with MMT were determined using a Zwick Roell (ZO10) with film sample of 22 mm in length and 5 mm in width at a cross-head speed of 10 mm/min at 25 °C (as per ASTM D882-95a).

3.4. Thermogravimetric analysis (TGA)

Thermogravimetric analyses of HPMC and its nanocomposite films were carried out on a Mettler-Toledo TGA/SDTA 851 thermal analyzer in a dynamic atmosphere of dinitrogen (flow rate = 30 cm^3 min^{-1}). The samples were heated in a alumina crucible at a rate of 10 °C/min over a temperature range of 50–500 °C.

3.5. Moisture absorption

The moisture absorption of HPMC and its nanocomposites films was determined by the following method. The film samples were cut in the dimension of 3 cm × 3 cm. Then samples were dried until constant weight in an oven at 60 °C to remove the moisture and immediately weighted as the initial weight (W_i). The samples were kept in a 75% constant relative humidity environment generated in a hermetic glass container with aqueous saturated NaCl solutions (Cyras, Manfredi, Ton-That, & Va'zquez, 2008) (ASTM E 104–85). After 24 h, the film samples were weighted immediately to obtaining final weight (W_f). Then, the moisture absorption of film samples were calculated by the following equation (Huang, Yu, & Ma, 2004):

$$\text{Moisture absorption } (\%) = \frac{W_f - W_i}{W_i} \times 100 \quad (2)$$

3.6. UV–vis spectroscopy

Optical clarity of the film samples were examined by UV–vis absorption spectrum. The film samples were performed in an Agilent 8453 Spectrophotometer, USA in the wave length range from 200 to 800 nm.

3.7. Water vapor transmission rate (WVTR)

Water vapor permeability of the layer silicate nanocomposite films was calculated in accordance with the modified ASTM E96-00 method (ASTM, 2000). Film samples were sealed over a 60 mm circular opening of a permeation cell containing calcium chloride (0% RH inside the cell). Then the permeation cells were placed inside a desiccator containing the saturated sodium chloride solution (75% RH outside the cell), to create a 75% RH gradient across the film (Cyras, Manfredi, That, & Va'zquez, 2011). The water vapor transport was determined from the weight gain of the permeation cell every 24 h until constant rate of weight gain was attained.

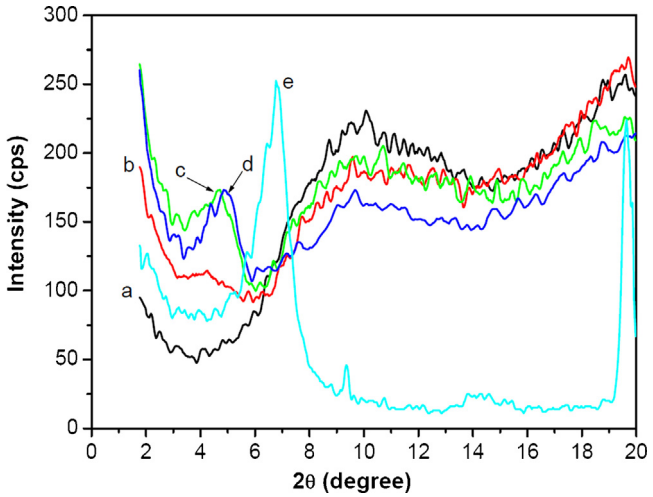

Fig. 1. XRD patterns of (a) HPMC, (b) HPMC/3 wt% Na^+MMT, (c) HPMC/5 wt% Na^+MMT, (d) HPMC/7 wt% Na^+MMT and (e) Na^+MMT.

Water vapor transmission rate was calculated by using the following equation (Mohd Amin, Abadi, Ahmad, Katas, & Jamal, 2012):

$$Q = \frac{WL}{S} \quad (3)$$

where W is increase in the desiccant weight per 24 h, L is the film thickness (cm), S is the exposed surface area (cm^2) and Q is the water vapor transmission rate ($g/cm^2/24\,h$).

4. Results and discussion

4.1. Morphology of nanocomposite films

X-ray diffraction (XRD) is an effective method to determine the state of intercalation/exfoliation of nanoclay in the polymer matrix. Fig. 1 shows the XRD patterns of pure HPMC, montmorillonite and nanocomposites of HPMC/MMT. The diffraction peak of pure MMT is observed at 6.75° corresponding to interlayer spacing of 1.308 nm. From Fig. 1, it is clear that pure HPMC has no peak in the range 2–10° and the diffraction peak of MMT shifts towards lower angle values in the HPMC/MMT nanocomposite films. The diffraction peak of HPMC/MMT nanocomposites is obtained at 4.21°, 4.69° and 4.90° corresponding to interlayer distance of 2.09 nm, 1.88 nm and 1.801 nm with loading of 3 wt%, 5 wt% and 7 wt% MMT respectively. Therefore, the results establish formation of intercalated HPMC/MMT nanocomposites due to strong polar interactions between the hydroxyl groups present in HPMC and in the silicate layers (Park et al., 2002). The intensity of the diffraction peak of MMT in HPMC/MMT nanocomposites increases with increasing percentage of MMT loading.

From the XRD results, it is clear that intercalated HPMC/MMT nanocomposites are formed and TEM analysis can be used to support XRD results. Fig. 2(a)–(f) shows TEM micrographs of HPMC/MMT nanocomposites. Dark lines are representing 1 nm thick clay sheets and the gap between two adjacent lines is the interlayer spacing or gallery spacing of MMT. Fig. 2a, c, and e shows the interlayer spacing of MMT in the polymer matrix at high magnification and Fig. 2b, d and f shows dispersion of clay layers at low magnification of HPMC/MMT nanocomposites with loading 3 wt%, 5 wt% and 7 wt% MMT respectively. Fig. 2a establishes the formation of partly intercalated and partly exfoliated nanocomposite of HPMC/3 wt% MMT. The interlayer spacing of HPMC/3 wt% MMT

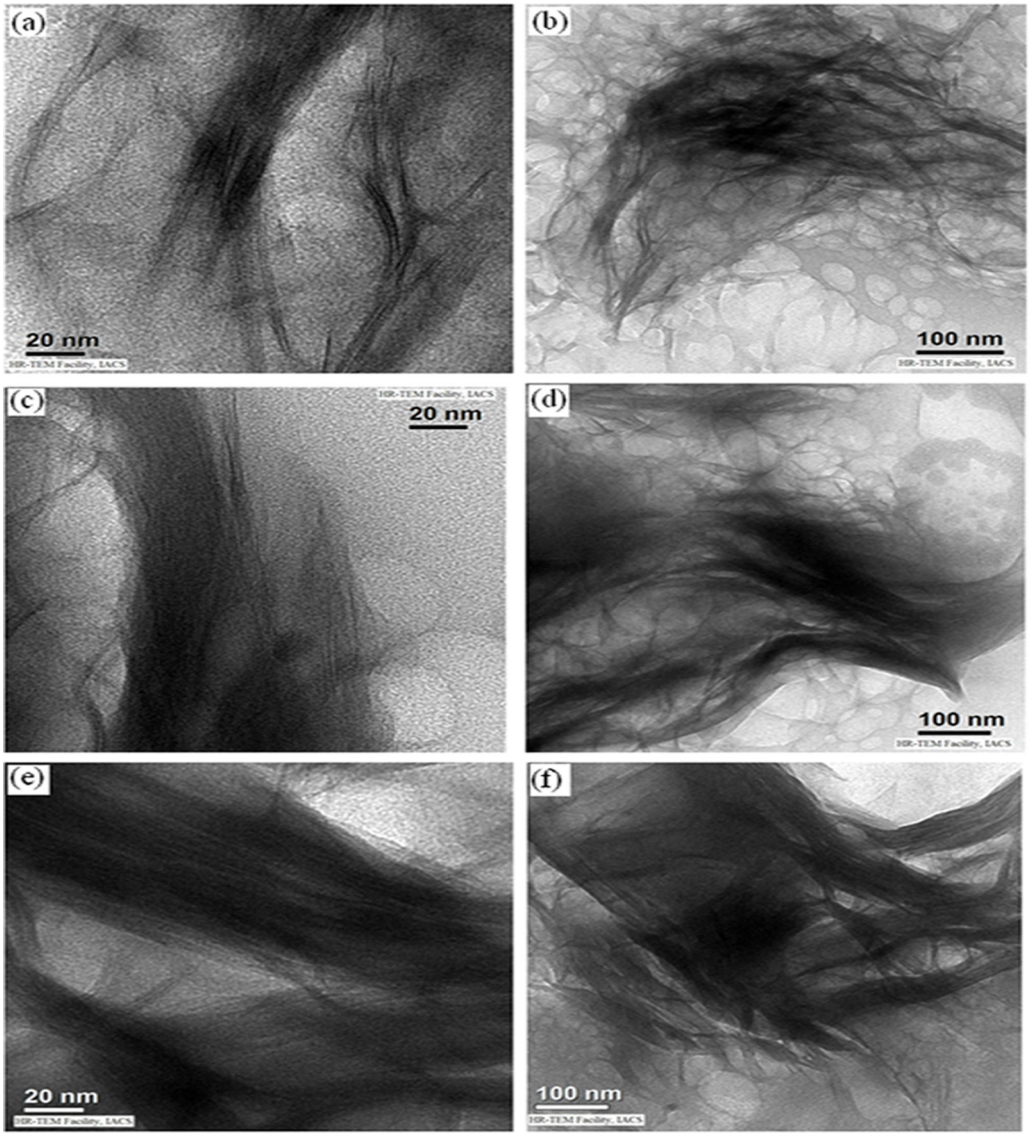

Fig. 2. TEM images of HPMC/Na^+MMT nanocomposites. (a and b) HPMC/3 wt% Na^+MMT nanocomposite at high and low magnification. (c and d) HPMC/5 wt% Na^+MMT nanocomposite at high and low magnification. (e and f) HPMC/7 wt% Na^+MMT nanocomposite at high and low magnification.

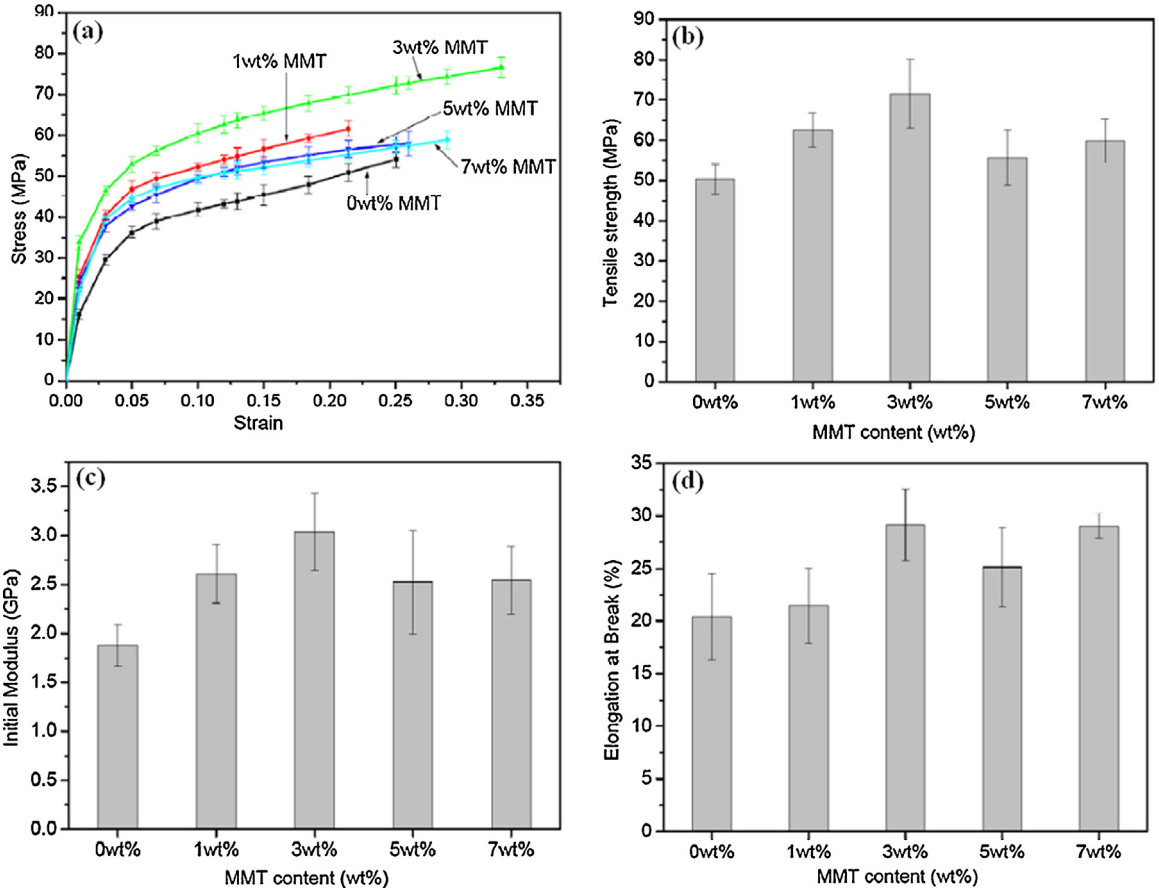

Fig. 3. Variation of (a) stress–strain curve, (b) tensile strength, (c) initial tensile modulus (0.01% strain) and (d) elongation at break of HPMC/MMT nanocomposite films at different concentration of MMT.

nanocomposites is measured from Fig. 2a and is found 2.21 nm which is close to XRD results. Fig. 2b shows that MMT layered silicates are well dispersed in the HPMC matrix with some degree of agglomeration. It is clear from Fig. 2b, d and f, the degree of agglomeration of MMT increases with increasing concentration of MMT from 3 wt% to 5 wt% and 7 wt% MMT.

4.2. Mechanical properties of nanocomposite films

Fig. 3a shows the stress–strain curve of HPMC/MMT nanocomposites. From Fig. 3a, tensile strength, tensile modulus and % elongation are calculated and plotted. Fig. 3b shows the tensile strength of films of HPMC and its nanocomposites with different percentage of MMT loading. It is clear from Fig. 3b that the tensile strength of pure HPMC film is improved from 50.2 MPa to 62.6 MPa and 71.6 MPa with loading of 1 wt% and 3 wt% MMT respectively. That means the tensile strength is increased by 24.70% and 42.63% with loading of 1 wt% and 3 wt% MMT respectively and this improvement can be correlated to the partly exfoliated and partly intercalated morphology of the HPMC/MMT nanocomposite films. It is also observed that with increasing the loading of MMT from 3 wt% to 5 wt% and 7 wt% in the HPMC matrix, the tensile strength increases by 10.96% and 19.32% respectively. Therefore, it can be concluded that HPMC/3 wt% MMT nanocomposite is the best combination for getting maximum tensile strength. At higher percentage of MMT, the improvement is not as much as in case of 3 wt% and that may be due to the more agglomeration of MMT layers in the nanocomposite films.

Fig. 3c shows the tensile modulus at 0.01% stain of HPMC and its nanocomposite films with loading of various percentage of MMT. The tensile modulus of pure HPMC film increases from 1.875 GPa to 2.61 GPa and 3.039 GPa with loading of 1 wt% and 3 wt% MMT respectively. Therefore, the tensile modulus is increased by 62.08% with loading of 3 wt% MMT. This remarkable improvement of tensile modulus is due to partly exfoliated and partly intercalated morphology of HPMC/3 wt% MMT nanocomposite films which is clear from XRD results. According to Giannelis et al. this remarkable improvement can be thought of as the region of the polymer matrix that is physisorbed on the silicate surface, and is thus stiffened through its affinity for adhesion to the filler surfaces (Shia, Hui, Burnside, & Giannelis, 1998). The tensile modulus of pure HPMC is enhanced by 34.57% and 35.79% with loading 5 wt% and 7 wt% MMT respectively. So, it can be concluded from above observation that HPMC/3 wt% MMT is the best composition for getting maximum improvement in tensile strength and tensile modulus.

Elongation at break of HPMC films with loading of various percentage of MMT is shown in Fig. 3d. The elongation at break of HPMC film increases with incorporation of MMT and the extent of increase is maximum in case of 3 wt% MMT. The elongation at break of HPMC is increased from 20.4% to 21.5%, 29.2%, 25.1% and 29% with loading 1 wt%, 3 wt%, 5 wt% and 7 wt% MMT respectively.

So, from the above observation it can be concluded that inclusion MMT not only responsible for strengthening but also toughening of HPMC matrix and maximum improvement is observed in case of HPMC/3 wt% MMT nanocomposite.

4.3. Thermal properties of nanocomposite films

Fig. 4(I) shows the thermal degradation of the pure HPMC and its nanocomposites films and the first order derivatives curves (DTG)

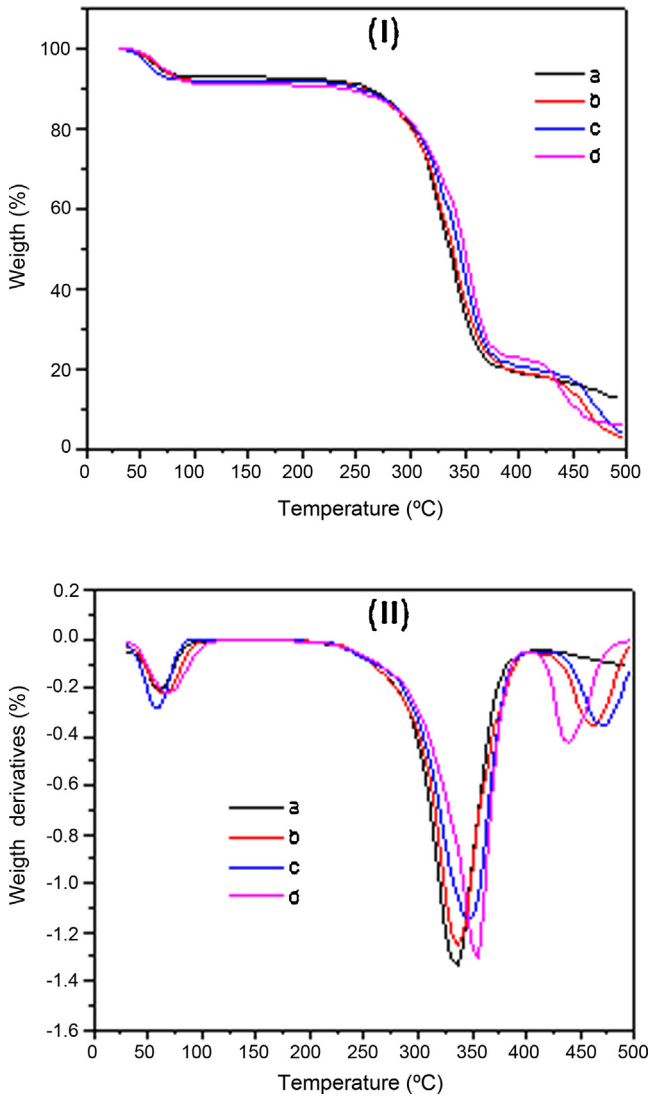

Fig. 4. (I) TGA and (II) DTG curves of (a) HPMC, (b) HPMC/3 wt% Na^+MMT, (c) HPMC/5 wt% Na^+MMT and (d) HPMC/7 wt% Na^+MMT.

of weight loss as a function of temperature are shown in Fig. 4(II). The first weight loss observes approximately between 50 °C and 90 °C for all samples due to presence of moisture and high water retention capacity of HPMC which is similar to a reported work on methylcellulose (MC) systems (Rimdusit et al., 2008). The major weight losses are observed in the range of 250–400 °C, which corresponds to the structural decomposition of the HPMC. From the Fig. 4(I), it is clear that the thermal decomposition of pure HPMC is shifted towards higher temperature with addition of MMT. Therefore, the thermal stability of the HPMC is enhanced in presence of MMT because MMT layers act as barriers to maximize the heat insulation and to minimize the permeability of volatile degradation products through the material (Chang et al., 2003). The temperature of half-way degradation (the temperature at which 50% of the sample weight is lost) of pure HPMC film is increased from 335 °C to 338 °C, 343 °C and 349 °C with addition of 3 wt%, 5 wt% and 7 wt% MMT respectively. Fig. 4(II) shows that the maximum degradation temperature (the temperature at which maximum weight loss occurs) of HPMC increases from 334 °C to 337 °C with loading of 3 wt% MMT. It is further observed that with the addition of 5 wt% and 7 wt% MMT in the HPMC matrix, the maximum degradation temperature again increases to 346 °C and 355 °C, respectively.

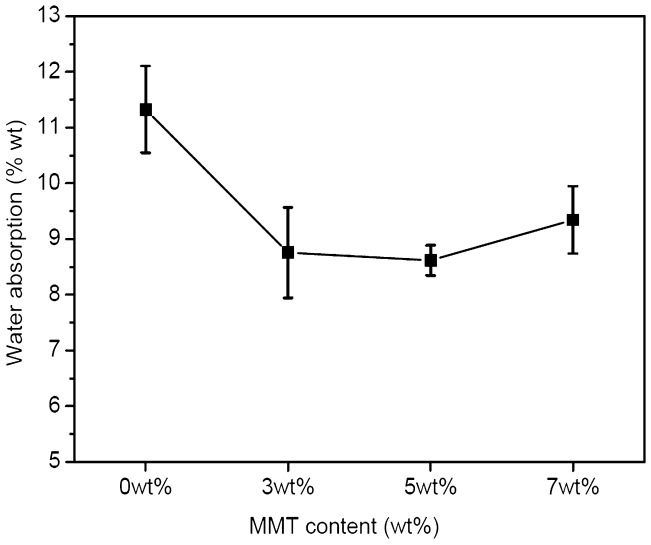

Fig. 5. Moisture absorption (%) of HPMC/MMT nanocomposite films at various contents of MMT.

4.4. Moisture absorption of nanocomposite films

Fig. 5 shows the moisture absorption of HPMC and its nanocomposite films. The moisture absorption of HPMC films decreases with loading of MMT due to the formation of hydrogen bonds between HPMC and MMT. For this reason, free water molecules do not interact as strongly as with HPMC/MMT nanocomposite films as with HPMC film alone (Carvalho, Curvelo, & Agnelli, 2001; Huang et al., 2004). Moisture absorption of pure HPMC is 11.33% in 73% relative humidity at 20 °C. It is observed that with loading of 3 wt% MMT in the HPMC film matrix the moisture absorption decreases to 8.75% that means moisture absorption decreases by 22.77% compare to pure HPMC film. Cyras et al. (2008) have reported similar observation in case of starch/MMT nanocomposite where moisture absorption decreases by 19.23% compare to pure starch with the addition of 5 wt% MMT. It is further observed that the moisture absorption of pure HPMC does not alter much with the increasing concentration of MMT from 3 wt% to 7 wt%.

4.5. UV–vis spectroscopy analysis of nanocomposite films

Optical clarity of HPMC and its nanocomposite films are studied by UV–vis spectroscopy. Generally, exfoliated clay nanocomposites have higher optical clarity than phase separated composites (Gusev & Lusti, 2001; Schmidt & Malwitz, 2003) due to the presence of aggregated clay layers leading to strong scattering and/or absorption, resulting in very low transmission of the UV–vis light. The variation of transmittance of UV–vis light with wavelength is shown in Fig. 6. The % transmittance of pure HPMC film is not much affected at the visible range in presence of MMT. So, it can be concluded that maximum part of MMT is uniformly dispersed in HPMC matrix.

4.6. Water vapor transmission rate (WVTR) of nanocomposite films

Water vapor permeability of HPMC and its nanocomposite films are shown in Fig. 7. For packaging applications, permeability of film is most important factor and it should be better at lower value. The water vapor permeability of HPMC film decreases in presence of MMT due to the increase in path of diffusion which is schematically shown in Fig. 8. When 3 wt%, 5 wt% and 7 wt% MMT is incorporated into HPMC matrix, WVTR of HPMC decreases from 24.1×10^{-5}

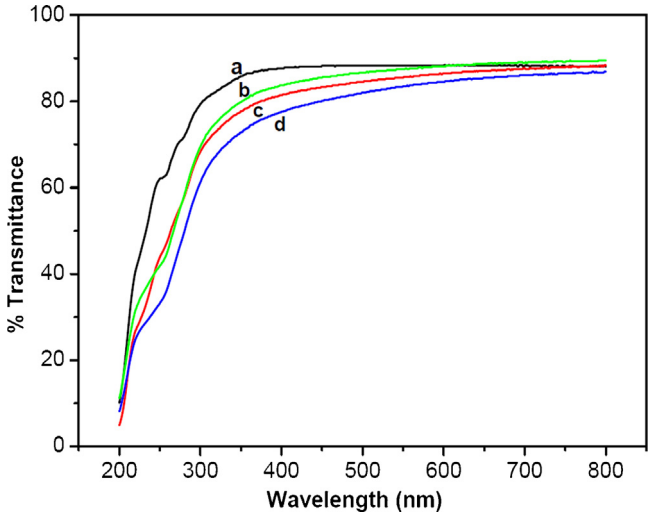

Fig. 6. The % of transmittance of (a) HPMC, (b) HPMC/3 wt% Na^+MMT, (c) HPMC/5 wt% Na^+MMT and (d) HPMC/7 wt% Na^+MMT against wavelength.

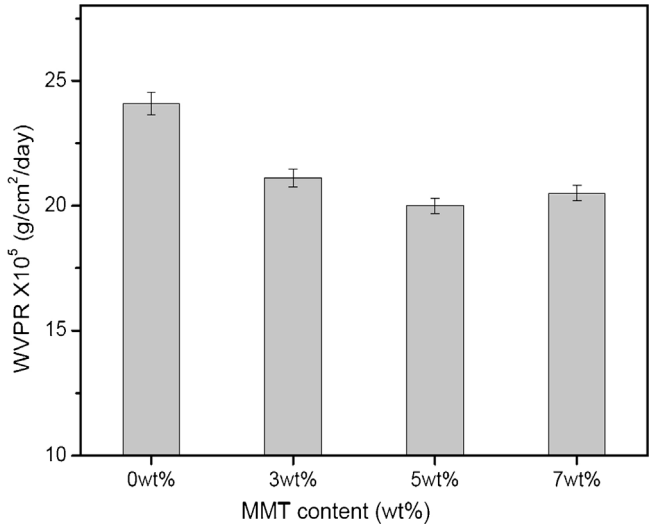

Fig. 7. Water vapor permeability rate (WVPR) of HPMC/MMT nanocomposite films at various contents of MMT.

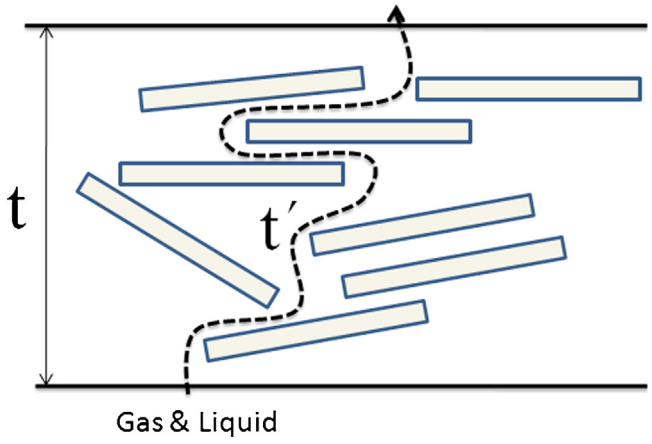

Fig. 8. Schematic model describing the path of the diffusing gas and liquid through the nanocomposite film (t and t' = tortuous path for diffusion).

to 21.1×10^{-5}, 20×10^{-5} and 20.5×10^{-5} g/cm^2/day respectively. Therefore, WVTR of HPMC decreases by 12.45%, 17.01% and 14.94% with the addition of 3 wt%, 5 wt% and 7 wt% MMT respectively. The increase in water vapor barrier property of polymer/clay composite films is mainly attributed to the tortuous path for water vapor diffusion due to the impermeable clay layers distributed in the polymer matrix increases the effective diffusion path length (Cussler, Highes, Ward, & Aris, 1998; Yano, Usuki & Okada, 1997). From Fig. 7, it is also clear that with the addition of more nanoclay in the HPMC matrix, water vapor permeability does not improve farther (Chiou et al., 2007; Park et al., 2002).

5. Conclusion

HPMC/MMT nanocomposites were prepared by solution casting method. XRD results established formation of intercalated nanocomposites. It was clear from TEM images that partly exfoliated and partly intercalated nanocomposite was formed in case of HPMC/3 wt%MMT combination. Tensile strength, tensile modulus and elongation at break of HPMC were improved with loading MMT. So, it can be concluded that inclusion of MMT not only responsible for strengthening but also toughening of HPMC matrix and maximum improvement was observed in case of HPMC/3 wt% MMT nanocomposite. The thermal stability of pure HPMC was increased with addition of MMT because MMT layers act as barriers to maximize the heat insulation. The amount of moisture absorption of pure HPMC film was reduced as free water molecules did not interact as strongly as with HPMC/MMT nanocomposite films as with HPMC film alone. The water vapor permeability of HPMC also decreased with addition of MMT which is important from packaging application point of view.

Acknowledgements

D. Mondal likes to thank the Council of Scientific & Industrial Research (CSIR), Govt. of India for his fellowship. B. Bhowmick likes to thank the Centre for Nanoscience and Nanotechnology, University of Calcutta. Md M.R. Mollick likes to thank Department of Science & Technology (DST), Govt. of India for his fellowship, and D. Maity likes to thank the University Grant Commission, Govt. of India for her fellowship.

References

Arvanitoyannis, I., Biliaderis, C. G., Ogawa, H., & Kawasaki, N. (1998). Biodegradable films made from low density polyethylene (LDPE), rice starch, and potato starch for food packaging applications. Part 1. *Carbohydrate Polymers*, *36*(2), 89–104.

ASTM. (2000). Standard test methods for water vapor transmission of material – E-96-00. In Annual Book of ASTM Standards. ASTM International, Philadelphia, USA.

Bhattacharya, M. (1998). Stress relaxation of starch/synthetic polymer blends. *Journal of Materials Science*, *33*(16), 4131–4139.

Carvalho, A. J. F., Curvelo, A. A. S., & Agnelli, J. A. M. (2001). A first insight on composites of thermoplastic starch and kaolin. *Carbohydrate Polymers*, *45*(2), 189–194.

Chang, J. H., Jang, T. G., Ihn, K. J., Lee, W. K., & Sur, G. S. (2003). Poly(vinyl alcohol) nanocomposites with different clays: Pristine clays and organoclays. *Journal of Applied Polymer Science*, *90*(12), 3208–3214.

Chiou, B. S., Wood, D., Yee, E., Imam, S. H., Glenn, G. M., & Orts, W. J. (2007). Extruded starch-nanoclay nanocomposites: Effects of glycerol and nanoclay concentration. *Polymer Engineering and Science*, *47*(11), 1898–1904.

Coffin, D. R., Fishman, M. L., & Cooke, P. H. (1995). Mechanical and microstructural properties of pectin starch films. *Journal of Applied Polymer Science*, *57*(6), 663–670.

Cussler, E. L., Highes, S. E., Ward, W. J., & Aris, R. J. (1998). Barrier membranes. *Journal of Membrane Science*, *38*(2), 161–174.

Cyras, V. P., Manfredi, L. B., Ton-That, M. T., & Va'zquez, A. (2008). Physical and mechanical properties of thermoplastic starch/montmorillonite nanocomposite films. *Carbohydrate Polymers*, *73*(1), 55–63.

Cyras, P. V., Manfredi, B. L., That, T. T. M., & Va'zquez, A. (2011). Properties of extruded xanthan–starch–clay nanocomposite films. *Brazilian Archives of Biology and Technology*, *54*(6), 1223–1333.

Gusev, A. A., & Lusti, H. R. (2001). Rational design of nanocomposites for barrier applications. *Advanced Materials*, *13*(21), 1641–1643.

Huang, M. F., Yu, J. G., & Ma, X. F. (2004). Studies on the properties of montmorillonite-reinforced thermoplastic starch composites. *Polymer*, *45*(20), 7017–7023.

Kampeerapappun, P., Aht-ong, D., Pentrakoon, D., & Srikulkit, K. (2007). Preparation of cassava starch/montmorillonite composite film. *Carbohydrate Polymers*, *67*(2), 155–163.

Mohd Amin, M. C. I., Abadi, G. A., Ahmad, N., Katas, H., & Jamal, J. A. (2012). Bacterial cellulose film coating as drug delivery system: Physicochemical, thermal and drug release properties. *Sains Malaysiana*, *41*(5), 561–568.

Park, H. M., Li, X., Jin, C. Z., Park, C. Y., Cho, W. J., & Ha, C. K. (2002). Preparation and properties of biodegradable thermoplastic starch/clay hybrids. *Macromolecular Materials and Engineering*, *287*(8), 553–558.

Ray, S. S., & Bousmina, M. (2005). Biodegradable polymers and their layered silicate nanocomposites: In greening the 21st century materials world. *Progress in Materials Science*, *50*(8), 962–1079.

Rimdusit, S., Jingjid, S., Damrongsakkul, S., Tiptipakorn, S., & Takeichi, T. (2008). Biodegradability and property characterizations of methyl cellulose: Effect of nanocompositing and chemical crosslinking. *Carbohydrate Polymers*, *72*(3), 444–455.

Romero, R. B., Leite, A. P. C., & Gonçalves, M. C. (2009). The effect of the solvent on the morphology of cellulose acetate/montmorillonite nanocomposites. *Polymer*, *50*(1), 161–170.

Schmidt, G., & Malwitz, M. M. (2003). Properties of polymer–nanoparticle composites. *Current Opinion in Colloids and Interface Science*, *8*(1), 103–108.

Shia, D., Hui, C. Y., Burnside, S. D., & Giannelis, E. P. (1998). An interface model for the prediction of Young's modulus of layered silicate–elastomer nanocomposites. *Polymer Composites*, *19*(5), 608–615.

Simkovic, I., Laszlo, J. A., & Thompson, A. R. (1996). Preparation of a weakly basic ion exchange by crosslinking starch with epichlorohydrin in the presence of NH_4OH. *Carbohydrate Polymers*, *30*(1), 25–30.

Tang, X., & Alavi, S. (2012). Structure and physical properties of starch/polyvinyl alcohol/laponite RD nanocomposite films. *Journal of Agricultural and Food Chemistry*, *60*(8), 1954–1962.

Tunç, S., & Duman, O. (2007). Thermodynamic properties and moisture adsorption isotherms of cottonseed protein isolate and different forms of cottonseed samples. *Journal of Food Engineering*, *81*(1), 133–143.

Tunç, S., & Duman, O. (2010). Preparation and characterization of biodegradable methyl cellulose/montmorillonite nanocomposite films. *Applied Clay Science*, *48*(3), 414–424.

Wang, S. F., Shen, L., Tong, Y. J., Chen, L., Phang, I. Y., Lim, P. Q., et al. (2005). Biopolymer chitosan/montmorillonite nanocomposites: Preparation and characterization. *Polymer Degradation and Stability*, *90*(1), 123–131.

Xu, Y. X., Kim, K. M., Hanna, M. A., & Nag, D. (2005). Chitosan-starch composite film: Preparation and characterization. *Industrial Crops Products*, *21*(2), 185–192.

Yang, K. K., Wang, L. X., & Wang, Y. Z. (2007). Progress in nanocomposite of biodegradable polymer. *Journal of Industrial and Engineering Chemistry*, *13*(4), 485–500.

Yano, K., Usuki, A., & Okada, A. (1997). Synthesis and Properties of Polyimide-Clay Hybrid Films. *Journal of Polymer Science Part A: Polymer Chemistry*, *35*(11), 2289–2294.